Pricing carbon emissions reduces health inequities from air pollution exposure

Xinyuan Huang[1,1], Vivek Srikrishnan[2,2], Jonathan Lamontagne[3,3], Klaus Keller[4,4], and Wei Peng[1,1]

[1]Penn State University
[2]Cornell University
[3]Tufts University
[4]Dartmouth College

November 30, 2022

Abstract

Climate mitigation can bring health co-benefits by improving air quality. Yet, whether mitigation will widen or narrow current health disparities remains unclear. Here we use a coupled climate-energy-health model to assess the effects of a global carbon price on the distribution of ambient fine particulate matter (PM2.5) exposure and associated health risks across an ensemble of nearly 30,000 future scenarios. We find that pricing carbon consistently lowers the PM2.5-attributable death rates in lower-income countries by reducing fossil fuel burning (e.g., China and India). Since these countries are projected to have large ageing populations, the greatest reduction in global average PM2.5-attributable death rate is found in elderly populations, which are more vulnerable to air pollution than the other age groups. In contrast, the health effects in higher-income countries are more complex, because pricing carbon can increase the emissions from bioenergy use and land-use changes, counteracting the mortality decrease from reduced fossil fuel burning. Mitigation technology choices and complex interactions between age structures, energy use, and land use all influence the distribution of health effects. Our results highlight the importance of an improved understanding of regional characteristics and cross-sector dynamics for addressing the interconnected challenges of climate, health, and social inequalities.

Pricing carbon emissions reduces health inequities from air pollution exposure

*Xinyuan Huang[1], Vivek Srikrishnan[2], Jonathan Lamontagne[3], Klaus Keller[4], Wei Peng[1,5]**

[1] Department of Civil and Environmental Engineering, The Pennsylvania State University, University Park, PA, USA.

[2] Department of Biological and Environmental Engineering, Cornell University, Ithaca, NY, USA.

[3] Department of Civil and Environmental Engineering, Tufts University, Medford, MA, USA.

[4] Thayer School of Engineering, Dartmouth College, Hanover, NH, USA.

[5] School of International Affairs, The Pennsylvania State University, University Park, PA, USA.

* Corresponding author: weipeng@psu.edu

Climate mitigation can bring health co-benefits by improving air quality[1,2]. Yet, whether mitigation will widen or narrow current health disparities remains unclear. Here we use a coupled climate-energy-health model to assess the effects of a global carbon price on the distribution of ambient fine particulate matter ($PM_{2.5}$) exposure and associated health risks across an ensemble of nearly 30,000 future scenarios. We find that pricing carbon consistently lowers the $PM_{2.5}$-attributable death rates in lower-income countries by reducing fossil fuel burning (e.g., China and India). Since these countries are projected to have large ageing populations, the greatest reduction in global average $PM_{2.5}$-attributable death rate is found in elderly populations, which are more vulnerable to air pollution than the other age groups. In contrast, the health effects in higher-income countries are more complex, because pricing carbon can increase the emissions from bioenergy use and land-use changes, counteracting the mortality decrease from reduced fossil fuel burning. Mitigation technology choices and complex interactions between age structures, energy use, and land use all influence the distribution of health effects. Our results highlight the importance of an improved understanding of regional characteristics and cross-sector dynamics for addressing the interconnected challenges of climate, health, and social inequalities.

Lowering fossil fuel burning reduces emissions of carbon dioxide as well as toxic air pollutants. As a result, climate mitigation efforts are expected to bring health co-benefits by improving air quality[2]. However, substantial pollution inequalities already exist between rich and poor nations. Half of the global total deaths attributable to fine particulate matter (technically $PM_{2.5}$) currently occur in China and India[3], due to high pollution levels and the large size of exposed population (i.e., 1/3 of the global population). The future health burden in these countries may decrease as air pollution control policies are further tightened to clean up the air, but could exacerbate if ageing trends increase the population's vulnerability to air pollution[4,5]. More importantly, how climate mitigation might improve or worsen the current disparities across countries remains poorly understood. Understanding the distribution of pollution and health effects is thus essential to identifying and addressing potential health inequities resulting from mitigation strategies[6].

The current evidence about the health implications of climate mitigation is mixed. Reducing fossil fuel combustion often lowers pollution exposure[2,7]. In densely populated countries, particularly those with large vulnerable populations, this reduced exposure results in a large decline in $PM_{2.5}$-attributable deaths[8]. However, energy mixes and socio-demographic patterns vary considerably across countries[9,10]. For instance, coal currently accounts for 67% of primary energy use (by EJ) in China, but only 25% in the US. Meanwhile, the size of the elderly population (age 65 or greater) is 131 million in China (9.5% of the national total population), as compared to 47 million in the US (15%)[4]. Hence, understanding the differential regional health impacts of climate mitigation requires careful consideration of the coupled energy and human systems[2,11]. Furthermore, changes in energy and socioeconomic patterns, which drive future pollution exposure and population vulnerability, are highly uncertain. These uncertainties pose considerable conceptual challenges for the assessment of future air pollution effects and the identification of key conditions that result in more or less equitable impact distributions.

Another factor complicating the seemingly straightforward link between climate mitigation and reduced mortality is the potential for new sources of air pollution to emerge as countries

transition towards low-carbon energy systems[12]. For instance, climate mitigation pathways may involve large-scale production and consumption of bioenergy[13]. This can increase the emissions of particulate matter from biomass combustion in end-use sectors[14] and the emissions of ammonia from upstream agricultural activities to produce bioenergy crops[15,16]. Besides the emissions from bioenergy production chains, bioenergy-heavy futures may also result in increased land competition[17], leading to additional emissions from land use changes (e.g., organic carbon emissions from burning forests[18]). This illustrates the complexities resulting from the multi-sector and multi-regional linkages which characterise global socioeconomic systems.

How will climate mitigation affect air pollution and health inequities in the 21st century? We start with a simple and widely discussed policy scenario: a globally uniform carbon price[19]. We link a leading integrated assessment model (Global Change Analysis Model, GCAM[20]) with a reduced-form air pollution model[21] and a country-level health impact assessment module[22]. We sample a wide range of uncertainties using nearly 30,000 scenarios covering a period from 2015 to 2100. By assessing the air quality and health impacts of carbon pricing for a large ensemble of future scenarios, our goal is to identify key socioeconomic and technological determinants for global pollution and health inequities.

We advance on the previous literature in three main ways. First, we expand on prior co-benefit studies by focusing on distributional outcomes. Equity considerations are central to the design of environmental policies in many societies[6]. Shifting from aggregate impacts to distributions is a crucial step towards analysing potential inequities.

Second, we build on previous work to consider a wide range of plausible futures. Our large-scale scenario ensemble approach provides a framework to incorporate uncertainties into the assessment of air quality and health outcomes in different world regions. Using the ensemble, we are able to evaluate quantitatively how various health pathways and system dynamics interact with each other under different assumptions of socioeconomic, technological, and agricultural uncertainties.

Third, we improve the process-based understanding of the complex pathways leading to varying health and equity outcomes (Figure 1). Climate mitigation induces changes in energy and land uses, which change the emissions of several air pollutants. How these emissions affect air quality is further affected by nonlinear atmospheric processes that determine pollution formation and wind transport. The resulting outcomes on human health are influenced by additional factors such as the location, size, and vulnerability of the exposed population. Importantly, along this pathway from health drivers to exposures and outcomes, the multi-sector, multi-regional economic and trade connections can result in unexpected spatial and temporal patterns. For instance, climate policies may reduce air pollution from fossil fuel combustion in some regions while increasing emissions from bioenergy consumption and production in other regions. Our integrated modelling framework allows us to characterise the relevant processes, with considerations of key uncertainties, and trace the influence of upstream drivers on downstream outcomes.

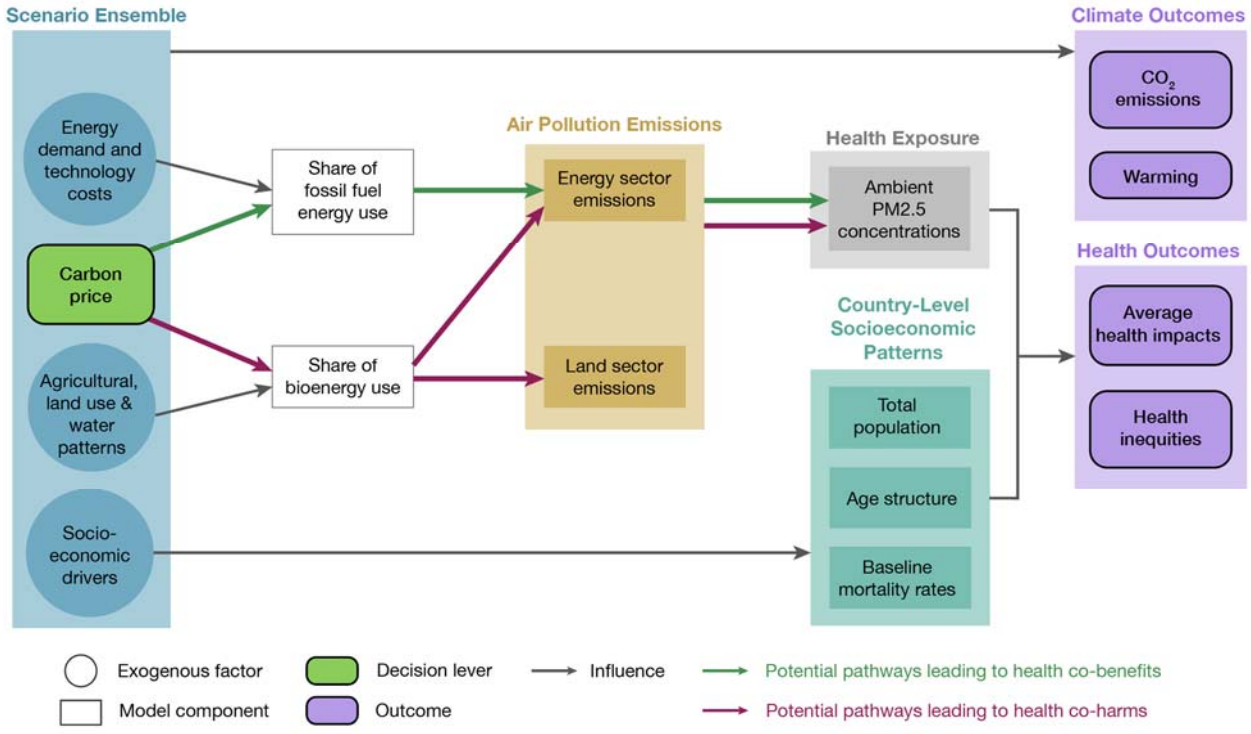

Figure 1. Potential health pathways for a global carbon price to influence regional pollution exposure and health outcomes. The green arrows illustrate a potential pathway for health co-benefits: carbon

pricing may reduce fossil energy use, which lowers precursor emissions and hence the ambient $PM_{2.5}$ concentrations. The red arrows illustrate a potential pathway for health co-harms: carbon pricing may increase bioenergy use, which increases emissions from energy and land use and hence ambient $PM_{2.5}$ concentrations. The scenario ensemble (N=28,706) samples uncertainties using the GCAM model[20]. We estimate the effects of air pollutant emissions on ambient $PM_{2.5}$ concentrations using the TM5-FASST model[21]. The health impact assessment further uses the projected population and age structure from the IIASA database[10] and the baseline mortality rates from the International Futures model[23]. More details are presented in the Method section.

A moderate carbon price trajectory lowers global warming and $PM_{2.5}$-attributable health risks

We impose a trajectory of carbon price on global energy sector CO_2 emissions to approximate moderate ambition level for climate action: $28, $69, and $117/ton CO_2 in 2030, 2050 and 2100, respectively (Figure 2a). The near-term price level reflects countries' Nationally Determined Contributions[24] and is broadly consistent with current policy trends[25,26]. The longer-term price level is in line with the required efforts to limit end-of-century warming to 2.1-4°C compared to pre-industrial global surface average temperature (or the radiative forcing level of roughly 4.5W/m^2)[27]. Compared to the no carbon price scenarios, we estimate that this carbon price trajectory reduces the global average temperature by 0.1°C (based on ensemble median; range 0.1–0.2°C across the considered scenarios) in 2050 and by 0.6°C (range: 0.5–0.8°C) in 2100 (Figure 2b).

Consistent with prior studies[1,7], we find that pricing carbon improves global air quality and reduces the average $PM_{2.5}$-attributable death rates. Based on the scenario ensemble considered in this study, globally, imposing the carbon price reduces the ensemble median $PM_{2.5}$-attributable death rate by 5% (or 33 deaths per million people; range: 18–51) in 2050 and 8% (or 77 deaths per million people; ensemble range: 28–169) in 2100 (Figure 2c). This corresponds to an annual average reduction of 0.2 (range: 0.1–0.5) million deaths from 2015 to 2100.

Pricing carbon reduces $PM_{2.5}$-related health inequities

In all scenarios, regional inequalities in pollution and health persist throughout the century. The future $PM_{2.5}$-attributable death rate remains higher in lower-income regions. For example, in scenarios without a carbon price, India and other South Asian nations have the highest $PM_{2.5}$-attributable death rates in 2050, with an ensemble median exceeding 750 deaths per million people. In contrast, the lowest projected death rates occur in Australia, Canada, and Northern Europe, with an ensemble median less than 200 $PM_{2.5}$-attributable deaths per million people.

Pricing carbon reduces, but does not eliminate, the regional inequities. The health benefits associated with the considered carbon price levels are greatest for lower-income regions (Figure 2d and Figure 3). For the high-risk, low-income regions, pricing carbon lowers the $PM_{2.5}$-attributable death rate by 53–90 deaths per million per year (or 5.6–7.3%) in India and other South Asian nations, based on the 2050 ensemble median. In comparison, for low-risk, high-income regions, the reduction is only 0.5–2.1 $PM_{2.5}$-attributable deaths per million per year (or 0.4–1.1%) in Australia, the United States, and Northern Europe.

Globally, the elderly population continues to be impacted most among all adult age groups from air pollution exposure. However, the considered carbon prices improve age-related inequities in $PM_{2.5}$-attributable death rates. This is due to the larger elderly population in lower-income countries that benefits from the exposure reductions. For example, without a carbon price, the global median $PM_{2.5}$-attributable death rate in 2050 is ten times higher for the 65 or older age group than the rest of the adult population (i.e., 25–64 years old; Figure 3). With a carbon price, the $PM_{2.5}$-attributable death rate is lowered by 92 deaths per million per year (or 5%) in the 65 or older age group, as compared to only 9 $PM_{2.5}$-attributable deaths per million per year (or 4%) for the rest of the adult population.

Pricing carbon provides a promising avenue to narrowing current pollution and health inequities, both across regions and across age groups. This core insight is largely consistent for all future

time periods, including mid-century as well as the end-of-century (see Supplementary Figure S1 for results for 2100).

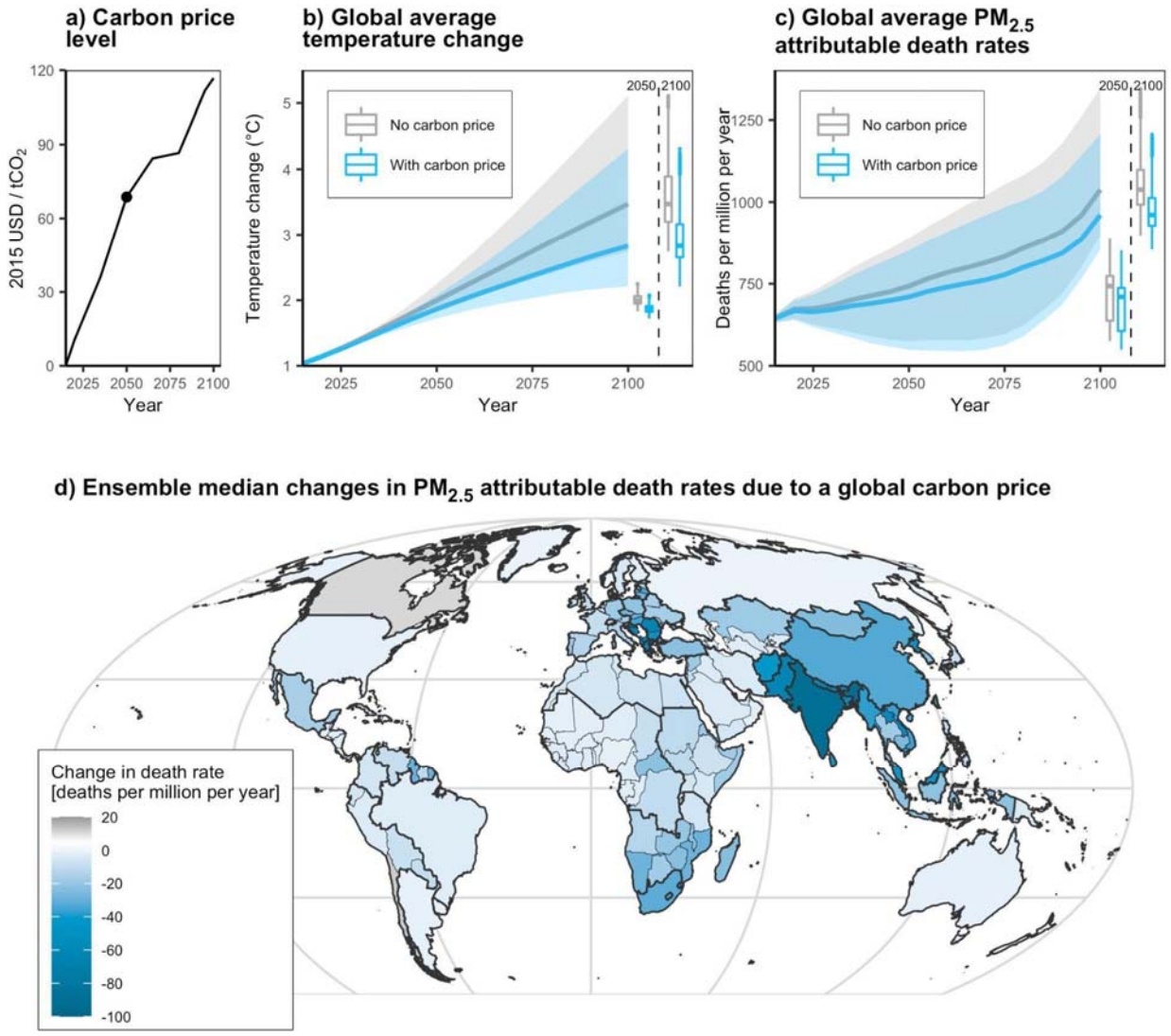

Figure 2. Impacts of a global carbon price on future global average temperature and regional distribution of $PM_{2.5}$-attributable death rates. Panel a) shows the carbon price trajectory from 2015 to 2100 considered in this study; the black dot highlights the price level in 2050 ($69/ton CO_2). Panels b) and c) present the global average temperature increase relative to the 1850 level and the annual $PM_{2.5}$-attributable death rates, including the median and ranges of the scenarios with and without a carbon price (N=14,180 and 14,526, respectively). Here the sample sizes are different because some combinations of input assumptions result in infeasible solutions (see Supplementary Information section 1.2 for more details). The box and whisker plots on the far right show the ensemble distributions in 2050

and 2100. Panel d) shows the 2050 regional changes in ensemble median $PM_{2.5}$-attributable death rate due to the carbon price (N=13,936; limiting to the pairs of scenarios that have feasible solutions in both cases). See Supplementary Figure S2 for the spatial distribution for 2100. We simulate the precursor emissions of air pollutants for 32 GCAM regions (shown as thicker borderlines, except Antarctica). We analyse health impact assessment for 178 regions and countries (shown as lighter borderlines), using downscaled emissions, simulated pollution levels, and socio-demographic information. We estimate the $PM_{2.5}$-attributable death rates using the median relative risks values from the Global Burden of Disease study[3].

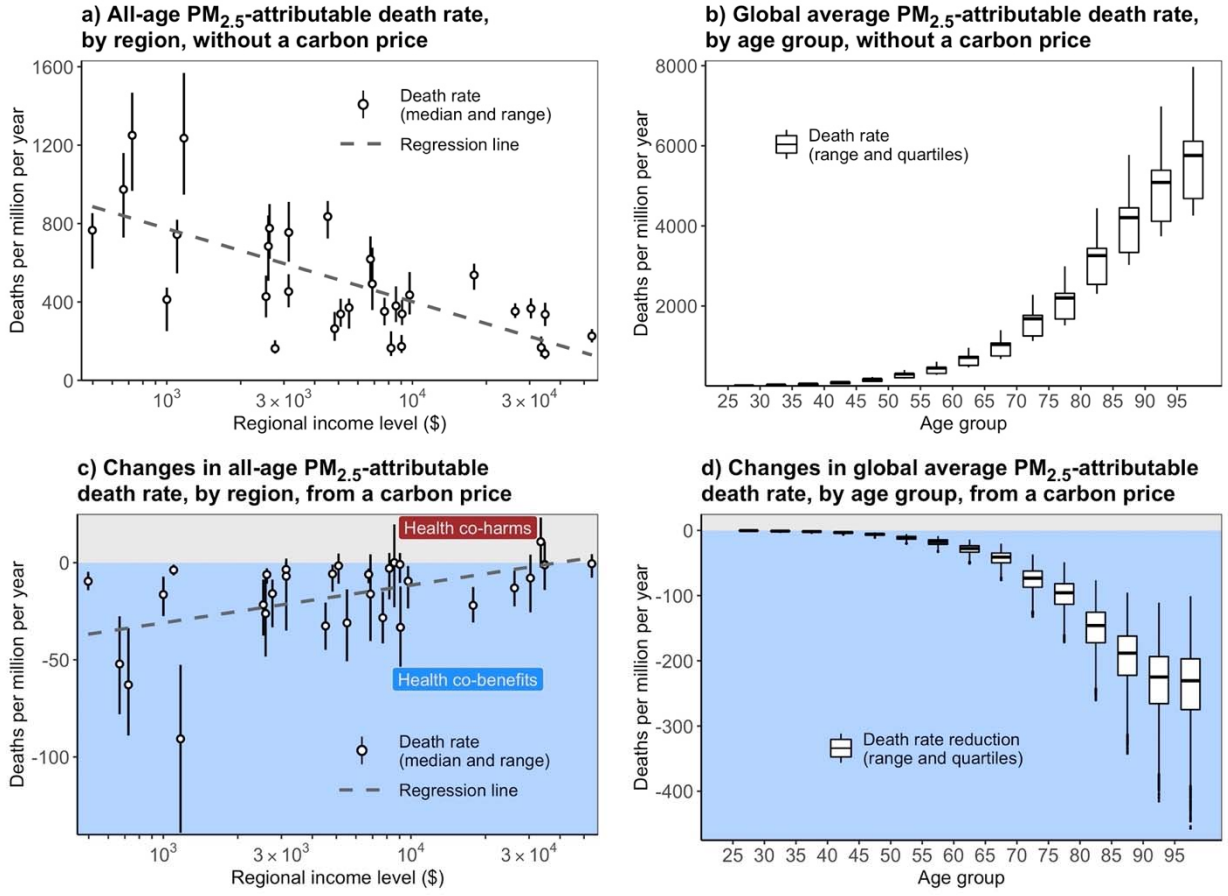

Figure 3. Distribution of $PM_{2.5}$-attributable death rates across regions and age groups in 2050. Panels a) and b) show the $PM_{2.5}$-attributable death rate without the carbon price, while panels c) and d) depict the changes in death rate due to a global carbon price of $69/ton. Panel a) and c) illustrate the variation in all-age $PM_{2.5}$-attributable death rate across world regions, ranked from low to high per capita income in 2015 (from left to right). The circles and error bars represent the scenario medians and ranges (N=13,936). Panel b) and d) show the variation in global average $PM_{2.5}$-attributable death rate across

adult age groups, ranked by 5-year groups from 25–29 to 95+ years old (from left to right). The box plots show the scenario medians, quartiles, and ranges (N=13,936). See Supplementary Figure S1 for the results for 2100.

Competing health pathways from carbon pricing

What causes these differential regional health effects of a global carbon price? Our analysis framework contains approximations for potential pathways through which a carbon price can result in co-benefits and co-harms. *Health co-benefits* can be driven by a reduction in air pollutant emissions from fossil fuel combustion, which is the dominant impact in lower-income regions. *Health co-harms* can result from increasing emissions from bioenergy use and land use changes associated with bioenergy production, which is more prominent in higher-income regions than lower-income regions. In our analysis, the relative importance of these two pathways contributes to the regional variations in how a global carbon price affects local emissions and pollution exposure. The health outcomes are further influenced by variations in population vulnerability (e.g., driven by age differences). We discuss these linkages in turn.

First, imposing the carbon price lowers fossil fuel uses and increases bioenergy uses across all world regions (Figure 4a). Yet, these changes depend on the current energy structures and projected technology costs. For instance, in 2050, the carbon price lowers the share of coal in the primary energy mix by 14 percentage points in India (based on ensemble median; range: 11–17), but only 5 percentage points in Canada (range: 3–7). This is consistent with the observation that India currently relies more heavily on coal (coal contributes 44% of its primary energy use[9]). The carbon price hence leads to a greater reduction in coal use in the model. In comparison, we find the increases in bioenergy shares are comparable across countries (e.g., increases by 2–5 percentage points across the six selected world regions, based on the ensemble medians). Here the small regional variations are largely driven by limited cross-region differences in bioenergy shares in current energy mixes, as well as in future bioenergy supply curves assumed in the model.

How changes in energy use affect air pollutant emissions depends on which sectors are being affected and the stringency of pollution regulation in relevant sectors (Figure 4b). For instance, carbon pricing leads to similar percentage reductions in coal share in Southeast Asia and the United States. Yet, the resulting reduction in per capita sulphur dioxide (SO_2) emissions is smaller in the US due to more stringent pollution control policies on existing coal facilities[28].

In addition, as a result of increased bioenergy use from carbon pricing, most countries are expected to slightly increase their organic carbon (OC) emissions, primarily due to bioenergy combustion in the residential/commercial sector (Figure 4b; see residential/commercial OC emissions in Supplementary Figure S6). In contrast, we find a much greater increase in OC emissions in Canada, where increased biomass production intensifies land competition and increases deforestation in unmanaged forest land (see per capita land use changes in Supplementary Figure S5). These results highlight that, under climate mitigation, air pollutant emissions can go up from new sources, including direct emissions from bioenergy combustion as well as indirect changes in land-use emissions arising from energy-land interactions.

Finally, regional socio-demographic characteristics affect population vulnerability, influencing health outcomes. For instance, the carbon price scenarios show larger relative increases in Canadian $PM_{2.5}$-attributable death rates than the associated $PM_{2.5}$ exposure levels. This is consistent with the combined effect of two factors: (i) nonlinear concentration-response relationships, which result in greater increases in mortality risks, from one unit increase in $PM_{2.5}$ exposure, in locations like Canada where the air is already relatively clean (see $PM_{2.5}$ concentrations without the carbon price in Supplementary Figure S7), and (ii) increased population ageing and hence vulnerability, which is expected to continue in advanced economies such as Canada (see Supplementary Table S5 for the age structures in each region).

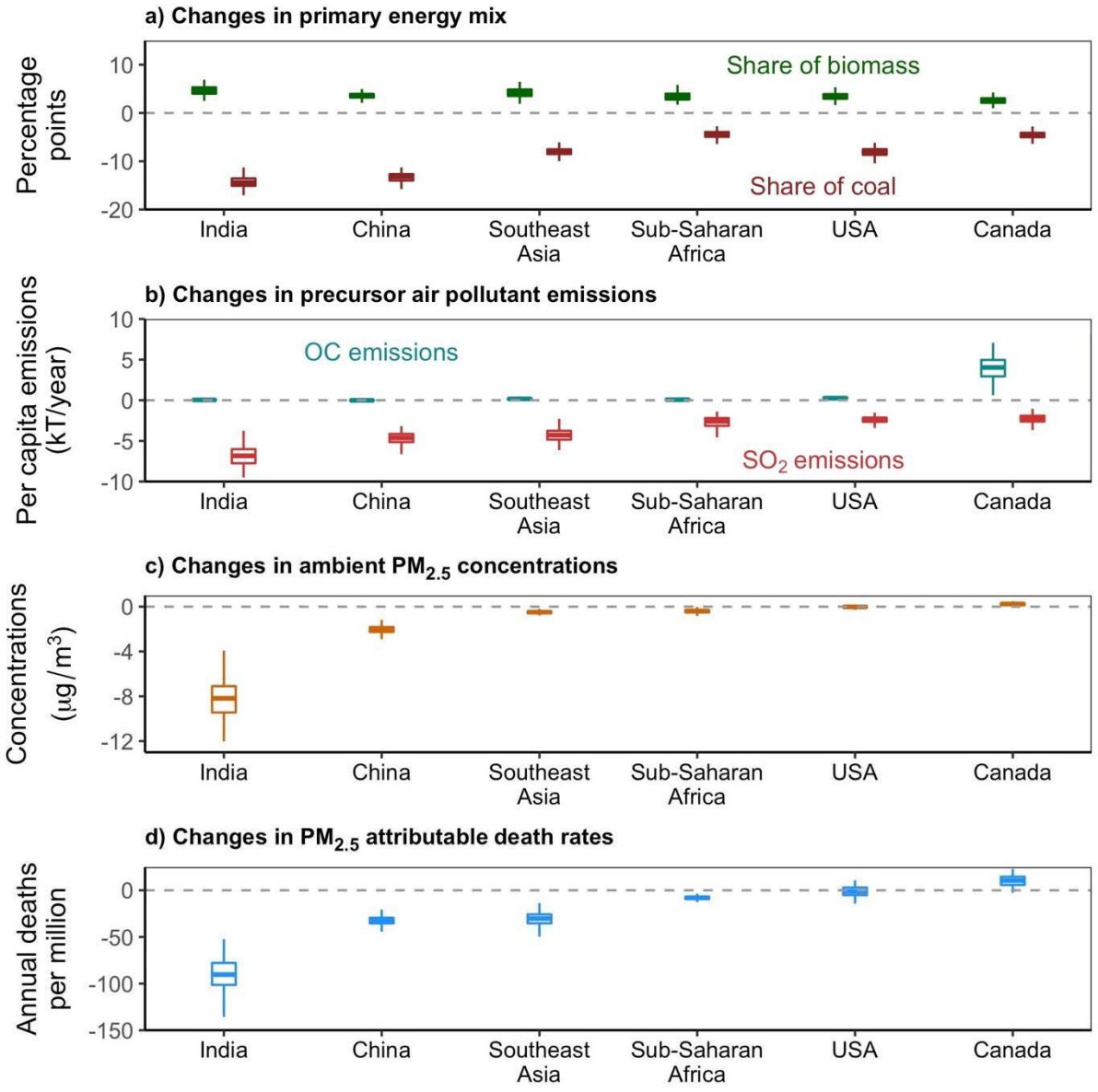

Figure 4. Regional changes in the health drivers, exposures, and risks as a result of the considered global carbon price in 2050. Here we include two lower-income regions (Sub-Saharan Arica and Southeast Asia), two fast-growing developing regions (China and India), and two developed countries (the United States and Canada) as the representative regions. Panel a) shows the changes (by percentage points) in shares of coal and biomass in the primary energy mix (See Supplementary Figure S8 for global regional-level distributions). Panel b) shows the changes in organic carbon (OC) and sulphur dioxide (SO_2) emissions per capita per year (see Supplementary Figure S4 for the scale of the small increases in the five regions on the left more clearly, and Supplementary Figure S9 for global regional-level distributions). Panels c) shows the changes in annual average $PM_{2.5}$ concentrations (see Supplementary Figure S10 for global regional-level distributions, and panel d) shows the changes in $PM_{2.5}$-attributable death rates. The

box and whiskers show the ensemble median, quartiles, and range. See Supplementary Figure S3 for the results for 2100.

Discussion

Our study illustrates how reducing fossil fuel combustion can affect global health outcomes. Greater decreases in $PM_{2.5}$-attributable death rates occur in more vulnerable populations, such as those in lower-income regions and the elderly. Our core finding—that pricing carbon can reduce pollution and health inequality—is robust across a wide range of plausible futures that vary in socioeconomic trends, energy demand and technology costs, as well as agricultural and land-use patterns.

Our analysis highlights the complexity of the system dynamics through which climate mitigation can influence the distribution of pollution and health effects. While the health co-benefits from reducing fossil fuel use are well documented[2,7], we demonstrate possible ways that climate mitigation can increase air pollutant emissions and health risks in some regions[29]. The key pathway for co-harms identified in our study is that carbon pricing can increase particulate matter emissions, both from direct bioenergy combustion and, in a handful of countries, also from indirect land use changes such as deforestation. Prior studies also found intensified land use competition in future mitigation scenarios that rely heavily on bioenergy[17]. While those studies demonstrated the emerging risks on food security[30] and water stress[31], our results suggest that unintended consequences can also occur for air quality and health. It underscores the importance of comprehensive assessment for the sustainability implications of large-scale mitigation responses to climate change.

Examining the pathways for health co-harms are particularly relevant for advanced economies. Prior studies demonstrated that the potential for health co-benefits from fossil reduction is often smaller in advanced economies than in the Global South countries due to already stringent pollution standards on existing fossil-based facilities[28,32]. More importantly, considering the

potential energy-land interactions, our analysis suggests that health co-benefits from fossil reduction will become less prominent as countries advance towards decarbonization, while the potential health co-harms from the mitigation actions will become increasingly important. Of course, the links between large-scale climate mitigation, air pollution, and the distribution of associated health impacts are still shrouded in considerable uncertainties. Our study contributes to the assessment of those effects under uncertainties and quantitatively demonstrates how climate mitigation can influence health inequity by changing energy systems, land uses, as well as their interactions with the socio-demographic patterns.

Our study is still silent on many important questions. For example, how can more refined strategies help to better navigate the complex landscape of climate, economics, and health? A globally uniform carbon price is simple to model and has some appealing theoretical advantages[19]. However, real-world policies are more diverse and fragmented[33]. Regulations and sector-based measures are widely and typically adopted and nearly everywhere have a bigger impact on emission abatement than directly pricing carbon[34,35]. We hypothesise that these different policy designs and targeted sectors would have different distributional consequences. For instance, compared to a subsidy on rooftop solar systems, electrifying the transport sector may bring greater benefits to populations living near major roads, who are often disproportionately minorities and people of lower socioeconomic status[36]. In addition, the health co-harms identified in our analysis may also be mitigated by imposing land conservation policies along with a carbon price on energy-sector emissions[37].

A second open question is how much-needed improvements in the representations of health drivers, exposures, and outcomes would impact the conclusion. For instance, bioenergy is an important technology driver for the health co-harms observed in our study. Yet, our modelling approach only considers 12 land types for 384 land regions worldwide. A detailed, subnational representation of land-use patterns is essential to identify suitable land for bioenergy production and model the competition between different land-use purposes[38,39]. Assessing the disparities across socio-demographic groups, both for exposure and health outcomes, also

requires fine-scale pollution simulation and health impact assessment. While some studies are moving in this direction[40,41], research that quantifies these linkages at decision-relevant resolutions is still largely in its infancy. These efforts can help in the search for decarbonization strategies that can simultaneously reduce adverse health impacts and associated inequities.

Our study lays the foundation for future efforts to address these open questions and advance our scientific understanding of the coupled energy-land-energy systems. Our work also has important policy implications. We find robust evidence on the country-varying health effects of climate mitigation and identify potential cross-sector linkages (e.g., between energy and land) that may redistribute the impacts. These insights are critically important, both for the international community and individual countries, to incorporate health and equity considerations into their climate policy designs.

Methods

1. Construction of scenario ensemble

We construct a large-scale scenario ensemble using a leading global-scale process-based integrated assessment model, GCAM v5.4[20] (Table 1). We consider one policy lever, i.e., whether a globally uniform carbon price trajectory (Figure 2a) is implemented from 2020-2100. We then sample seven types of future uncertainties in socioeconomic, technological, and land-use aspects (Table 1). We deploy a full factorial experimental design across the seven factors to encompass a wide range of futures[42]. Among the seven, four of them (i.e., socioeconomics, energy demand, agricultural and land use, fossil fuel extraction costs) are sampled by considering five sets of assumptions that reflect the storylines of Shared Socioeconomic Pathways (SSPs)[10]. For the other three factors, we sample the future water runoffs using varying levels of ground water level and reservoir capacity, and we sample the future competitiveness of low-emission energy technologies and carbon capture and sequestration (CCS) technology using varying levels of projected costs. The quantitative assumptions for different SSPs and technology costs are reported in Lamontagne et al. 2018[42] and Calvin et al. 2017[43].

GCAM is a global-scale, multi-sector model with technology-rich representations of five systems and their interactions: energy, water, agriculture and land use, economy, and climate systems[20]. Based on varying input assumptions on socioeconomic drivers, technology costs, and policy ambition, GCAM simulates the behaviours and interactions between these systems and projects future patterns at five-year intervals in a partial equilibrium economic modelling framework. For the GCAM version used in this study (v5.4), the energy and economy sectors are modelled for 32 world regions; the land system is divided into 384 subregions; and the climate/physical Earth system is simulated by a reduced-form climate model, Hector[44], at the global scale.

Table 1. Overview of scenario ensemble construction in GCAM. The presence or absence of the global carbon price, along with seven future scenario design factors, are sampled with a full factorial experimental design. See Supplementary Table S1 for the number of feasible scenarios.

<table>
<tr><th>Policy lever</th><th colspan="7">Future uncertainties</th></tr>
<tr><th>Carbon Price</th><th>Water runoff[a] (Groundwater level/Reservoir capacity level)</th><th>Socio-economic</th><th>Energy demand</th><th>AGLU[b]</th><th>Fossil fuel costs</th><th>Low-emissions energy costs</th><th>CCS[c]</th></tr>
<tr><td rowspan="3">No</td><td>Low/low</td><td>SSP1</td><td>SSP1</td><td>SSP1</td><td>SSP1</td><td rowspan="2">Low</td><td rowspan="3">Low</td></tr>
<tr><td rowspan="2">Low/high</td><td>SSP2</td><td>SSP2</td><td>SSP2</td><td>SSP2</td></tr>
<tr><td>SSP3</td><td>SSP3</td><td>SSP3</td><td>SSP3</td><td rowspan="3">Mid</td></tr>
<tr><td rowspan="3">Yes</td><td>High/low</td><td>SSP4</td><td>SSP4</td><td>SSP4</td><td>SSP4</td><td rowspan="3">High</td></tr>
<tr><td rowspan="2">High/high</td><td rowspan="2">High</td></tr>
<tr><td>SSP5</td><td>SSP5</td><td>SSP5</td><td>SSP5</td></tr>
</table>

[a] Water runoff scenario includes levels of groundwater and reservoir capacity.

[b] AGLU: Agricultural and land use

[c] CCS: Deployment cost of carbon capture and sequestration technology

Using the full factorial experimental design, we experimented with 30,000 scenarios using the GCAM model (15,000 pairs of scenarios with/without a carbon price). However, some scenarios do not yield feasible solutions. For example, the socioeconomic assumption following SSP5 (fossil-fuelled development) is not compatible with AGLU assumption following SSP3 (regional rivalry). AGLU assumption elements following SSP3, including low agricultural technology development, restricted trade, lack of land use regulations, and low agricultural productivity are

formidable obstacles to achieving high-level socioeconomic developments following SSP5. As a result, we have 14,526 feasible scenarios without a carbon price and 14,180 feasible scenarios with a carbon price. Between these two groups, we further pair up the scenarios with the same assumptions for other uncertainties and identify 13,936 pairs of scenarios that only differ in the policy lever.

2. Assessment of emissions of greenhouse gases (GHGs) and air pollutants

We project future emissions of annual total GHG and air pollutants for 32 GCAM regions, by technology and fuel choice.

GHG emissions: We estimate CO_2 emissions from fossil fuel and limestone uses by multiplying GCAM-projected production and consumption activities with the technology-specific emission factors estimated from the Carbon Dioxide Information Analysis Center (CDIAC, which is a global inventory of historical carbon emissions from 1751 to 2017[45]). CO_2 emissions from land-use and land-cover change are estimated based on the areas of land use change and the carbon intensity of each land use type[46]. We also calculate emissions of non-CO_2 GHGs, including methane, nitrous oxide, and fluorinated gases by multiplying relevant activities with the emission factors from EPA 2019[47]. When a carbon price is imposed, the amount of CO_2-emitting activities would be adjusted based on a regional marginal abatement cost curve derived from the costs of available mitigation options in each region.

Air pollutant emissions: We estimate the emissions of five types of air pollutants, including ammonia (NH_3), nitrogen oxides (NO_x), sulphur dioxide (SO_2), black carbon (BC), and organic carbon (OC) for 32 GCAM energy-economy regions. The emissions are calculated by multiplying relevant activities projected by the model with the respective emission factors derived from historical data[20]. To account for the tightening of air pollution control policies over time, the future emission factors are adjusted based on a declining trend with increasing income[48]. We

401 also adjust the technology mix over time by assuming a higher penetration rate of less polluting
402 units[43,48]. Both adjustments vary across five SSPs.
403
404 ***3. Assessment of climate outcomes***
405 We model the climate system using the Hector model[44] which interacts with the other parts of
406 GCAM at every five-year time step. Hector is a reduced-form global climate carbon-cycle model,
407 representing the most essential global-scale Earth system processes. The inputs to Hector are
408 global total GHG emissions aggregated across all GCAM sectors and regions. Then, Hector
409 reports global average radiative forcing and temperature changes.
410
411 ***4. Assessment of ambient $PM_{2.5}$ concentrations***
412
413 To assess the ambient $PM_{2.5}$ concentrations from precursor emissions, we use the TM5-FASST
414 model[21], a reduced-form source-receptor model for 56 world regions. The performance of TM5-
415 FASST was evaluated in a prior publication[8] and demonstrates satisfying model capabilities in
416 estimating ambient $PM_{2.5}$ concentrations.
417
418 To map from GCAM to TM5-FASST regions, we first downscale the emissions for 32 GCAM
419 regions to 178 countries (see Supplementary Table S2 for GCAM sector mapping), by sector and
420 for 5 types of precursor emissions, using the country-to-region ratios based on the Emission
421 Database for Global Atmospheric Research (EDGAR) data[49] (see Supplementary Table S3 for
422 EDGAR sector mapping). We then re-aggregate country-level emissions to the 56 TM5-FASST
423 regions.
424
425 For each year and scenario, we estimate the $PM_{2.5}$ concentrations using the changes relative to
426 2000, as the base year, assuming linear relationship between emissions and $PM_{2.5}$
427 concentrations as well as additivity across all types of emissions and regions. Specifically, the
428 following equation is used:

$$C(y) = C_{base}(y) + \sum_{x}^{n_x} \sum_{i}^{n_i} A_i[x,y] \cdot \left[E_i(x) - E_{i,base}(x)\right]$$

where $C(y)$ and $C_{base}(y)$ are the ambient $PM_{2.5}$ concentration in receptor region y in a future year of interest and in 2000, respectively. $E_i(x)$ *and* $E_{i,base}(x)$ are the emissions of the air pollutant type i from a source region x in a future year of interest and in 2000, respectively. $A_i[x,y]$ is the source-receptor coefficient, capturing how the emissions of precursor air pollutant type i in source region x would influence the ambient $PM_{2.5}$ concentrations in receptor region y. n_x is the total number of source regions whose emissions affect the ambient $PM_{2.5}$ concentration in receptor region y, plus two additional sources, shipping, and aviation, that are not tied to a particular location. i is the index for the type of precursor emissions, which include ammonia (NH_3), nitrogen oxides (NO_x), sulphur dioxide (SO_2), black carbon (BC), and particulate organic matter (POM) that are estimated from GCAM. n_i is the total number of precursors that form ambient $PM_{2.5}$. The unit of the $PM_{2.5}$ concentration is $\mu g/m^3$, and the units of the emissions are $\mathrm{kTonne}/year$.

Since TM5-FASST model uses the year 2000 as the base year, the values for $E_{i,base}(x)$ are taken from the Representative Concentration Pathway (RCP) database for the year 2000 at $1° \times 1°$ resolution[21]; using 2000 emissions as input, $C_{base}(y)$ is estimated using a full chemical transport model TM5-CTM[50], also at a global $1° \times 1°$ resolution. The values in the source-receptor matrix A are derived from a series of perturbation runs that increase the precursor emissions by 20%, by precursor type and source region, and assess the implications on $PM_{2.5}$ concentrations in each receptor region.

5. Assessment of $PM_{2.5}$-attributable deaths

Following the approach in the Global Burden of Disease Study[3], we consider six disease that have found to be associated with long-term exposure to ambient $PM_{2.5}$, namely chronic obstructive pulmonary disease (COPD), diabetes mellitus type II (DB), ischemic heart disease (IHD), lung cancer (LC), lower respiratory infections (LRI), and stroke.

For each of the five-year age group from 0 to 95+ in each of the 178 countries, we calculate the premature deaths attributable to each of the considered six diseases using the following equation:

$$\Delta Mort = y_0 \cdot AF(c) \cdot Pop,$$

where y_0 is age- and disease-specific the baseline mortality rate; Pop is the size of the exposed population in each age group; AF is the attributable fraction, which changes with varying exposure levels to $PM_{2.5}$ concentration (c) in each region. Below we describe the data source and calculation methods for each parameter.

a) *Population (Pop)*

We use age-specific population projections from the IIASA SSP database[10]. The population projections are at country level, with five-year intervals from 2010 to 2100, and vary across the five SSPs.

b) *Baseline Mortality Rates (y_0)*

For future time periods, we use the age-specific baseline mortality rates for each country projected by the International Futures (IFs) model v7.64[23], which also vary across the five SSPs. The baseline mortality rates from IFs are projected based on the GDP per capita and education attainment level and calibrated using the GBD 2004 data for cardiovascular diseases, diabetes, malignant neoplasms, respiratory diseases, and respiratory infections. We map IF-reported rates onto the six considered diseases: For IHD and stroke, we use the rates for total cardiovascular disease from IF and multiply by the shares of IHD and stroke in total cardiovascular-disease-related deaths; for LC, we use the rates for malignant neoplasms; for COPD, we use the rates for respiratory disease; for LRI, we use the rates for respiratory infections, and for DB, we use the rates for diabetes. To check the validity of this mapping method, we compared the disease-specific baseline mortality rates calculated using our methods with the rates reported by the GBD study and found them to be largely consistent (see Supplementary Table S4 for the comparison).

c) *Attributable Fraction* (AF)

For each disease and age group, we calculate the attributable fractions using the following equation:

$$AF(c) = \frac{RR(c)-1}{RR(c)},$$

where c is the $PM_{2.5}$ concentration in each country for which we assume all countries within the same TM5-FASST region have the same exposure level. The relative risks (RR) are obtained from the GBD 2019 study[3] and derived from the Integrated Exposure–Response (IER) model[22] for the six types of diseases for the $PM_{2.5}$ exposure levels from 0 to 600 μg/m³. The RRs are age-specific for IHD and stroke (from 25 to 95+ at five-year intervals) and are for all age-groups for the other four diseases.

Table 2. Summary of input data for the health impact assessment

Variables	Definition	Variations across scenarios	Data Source
y_0	Baseline mortality rate: present and future annual mortality rate that vary across age groups, diseases, and regions	Vary across five SSPs	International Futures v7.64[23]
Pop	Exposed population for each 5-year group	Vary across five SSPs	Shared Socioeconomic Pathways (SSP) database[10], generated with IIASA-Wic POP model.
RR	Relative risks (RR) of disease d for the respective age groups at the $PM_{2.5}$ levels of c For IHD and stroke: Age-specific RR functions For COPD, LC, LRI, and DB: All-age RR functions	Same in all scenarios	GBD Study 2019[3]

c	Annual mean exposures of $PM_{2.5}$ concentration	Different in each scenario	Calculated using TM5-FASST[21] based on GCAM emissions

Data availability Statement

The dataset generated during and analysed in the current study is available from a public zenodo repository (https://doi.org/10.5281/zenodo.6975580).

Code availability Statement

The GCAM model is available for download from https://github.com/JGCRI/gcam-core. Detailed model documentation is available online at http://jgcri.github.io/gcam-doc/index.html. The TM5-FASST model is available at http://tm5-fasst.jrc.ec.europa.eu/. The codes we use to process the data, calculate the health impacts, and make the plots are available from a public zenodo repository (https://doi.org/10.5281/zenodo.6975580).

Author contribution

X.H., V.S., K.K. and W.P. designed the study and interpreted the data. V.S. and J.L. constructed the scenario ensemble. X.H. led the data analysis and produced the figures. All authors co-wrote the manuscript.

Acknowledgements

X.H. and W.P. acknowledge the support from the National Science Foundation under Grant No. 2125293. We also thank the seed grant support from Penn State Institutes of Energy and the Environment and Institute for Computational and Data Sciences. K.K. thanks Dartmouth

College for its support. We thank Erin Mayfield, Lee Lynd, and Skip Wishbone for their invaluable input.

All errors and opinions are those of the authors and not of the funding entities.

References

1. Anenberg, S. C. *et al.* Global Air Quality and Health Co-benefits of Mitigating Near-Term Climate Change through Methane and Black Carbon Emission Controls. *Environ. Health Perspect.* **120,** 831–839 (2012).
2. Driscoll, C. T. *et al.* US power plant carbon standards and clean air and health co-benefits. *Nat. Clim. Change* **5,** 535–540 (2015).
3. Murray, C. J. L. *et al.* Global burden of 87 risk factors in 204 countries and territories, 1990–2019: a systematic analysis for the Global Burden of Disease Study 2019. *The Lancet* **396,** 1223–1249 (2020).
4. Yang, H., Huang, X., Westervelt, D., Horowitz, L. & Peng, W. Socio-demographic factors shaping the future global health burden from air pollution. *Nat. Sustain.* (accepted).
5. Shetty, P. Grey matter: ageing in developing countries. *The Lancet* **379,** 1285–1287 (2012).
6. Friel, S., Marmot, M., McMichael, A. J., Kjellstrom, T. & Vågerö, D. Global health equity and climate stabilisation: a common agenda. *The Lancet* **372,** 1677–1683 (2008).
7. West, J. J. *et al.* Co-benefits of mitigating global greenhouse gas emissions for future air quality and human health. *Nat. Clim. Change* **3,** 885–889 (2013).
8. Markandya, A. *et al.* Health co-benefits from air pollution and mitigation costs of the Paris Agreement: a modelling study. *Lancet Planet. Health* **2,** e126–e133 (2018).
9. IEA. World Energy Outlook 2021, IEA, Paris https://www.iea.org/reports/world-energy-outlook-2021. (2021).
10. Riahi, K. *et al.* The Shared Socioeconomic Pathways and their energy, land use, and greenhouse gas emissions implications: An overview. *Glob. Environ. Change* **42,** 153–168 (2017).
11. Yang, H., Pham, A. T., Landry, J. R., Blumsack, S. A. & Peng, W. Emissions and Health Implications of Pennsylvania's Entry into the Regional Greenhouse Gas Initiative. *Environ. Sci. Technol.* **55,** 12153–12161 (2021).
12. Owusu, P. A. & Asumadu-Sarkodie, S. A review of renewable energy sources, sustainability issues and climate change mitigation. *Cogent Eng.* **3,** 1167990 (2016).

13. Hanssen, S. V. *et al.* The climate change mitigation potential of bioenergy with carbon capture and storage. *Nat. Clim. Change* **10,** 1023–1029 (2020).
14. Hill, J. *et al.* Climate change and health costs of air emissions from biofuels and gasoline. *Proc. Natl. Acad. Sci.* **106,** 2077–2082 (2009).
15. Masera, O. R., Bailis, R., Drigo, R., Ghilardi, A. & Ruiz-Mercado, I. Environmental Burden of Traditional Bioenergy Use. *Annu. Rev. Environ. Resour.* **40,** 121–150 (2015).
16. Skorupka, M. & Nosalewicz, A. Ammonia Volatilization from Fertilizer Urea—A New Challenge for Agriculture and Industry in View of Growing Global Demand for Food and Energy Crops. *Agriculture* **11,** 822 (2021).
17. Popp, A. *et al.* Land-use futures in the shared socio-economic pathways. *Glob. Environ. Change* **42,** 331–345 (2017).
18. Klimont, Z. *et al.* Global anthropogenic emissions of particulate matter including black carbon. *Atmospheric Chem. Phys.* **17,** 8681–8723 (2017).
19. Cramton, P., Ockenfels, A. & Stoft, S. An international carbon-price commitment promotes cooperation. *Econ. Energy Environ. Policy* **4,** 51–64 (2015).
20. Calvin, K. *et al.* GCAM v5.1: representing the linkages between energy, water, land, climate, and economic systems. *Geosci. Model Dev.* **12,** 677–698 (2019).
21. Van Dingenen, R. *et al.* TM5-FASST: a global atmospheric source–receptor model for rapid impact analysis of emission changes on air quality and short-lived climate pollutants. *Atmospheric Chem. Phys.* **18,** 16173–16211 (2018).
22. Burnett, R. T. *et al.* An Integrated Risk Function for Estimating the Global Burden of Disease Attributable to Ambient Fine Particulate Matter Exposure. *Environ. Health Perspect.* **122,** 397–403 (2014).
23. Hughes, B. B. *et al.* Projections of global health outcomes from 2005 to 2060 using the International Futures integrated forecasting model. *Bull. World Health Organ.* **89,** 478–486 (2011).
24. Fawcett, A. A. *et al.* Can Paris pledges avert severe climate change? *Science* **350,** 1168–1169 (2015).

25. Ou, Y. *et al.* Can updated climate pledges limit warming well below 2°C? *Science* **374,** 693–695 (2021).
26. IPCC, 2022: Climate Change 2022: Mitigation of Climate Change. Contribution of Working Group III to the Sixth Assessment Report of the Intergovernmental Panel on Climate Change. Cambridge University Press, Cambridge, UK and New York, NY, USA.
27. *IPCC, 2021: Climate Change 2021: The Physical Science Basis. Contribution of Working Group I to the Sixth Assessment Report of the Intergovernmental Panel on Climate Change. Cambridge University Press, Cambridge, United Kingdom and New York, NY, USA, In press,*.
28. Lee, J. S. H. *et al.* Toward clearer skies: Challenges in regulating transboundary haze in Southeast Asia. *Environ. Sci. Policy* **55,** 87–95 (2016).
29. Commane, R. & Schiferl, L. D. Climate mitigation policies for cities must consider air quality impacts. *Chem* **8,** 910–923 (2022).
30. Frank, S. *et al.* Reducing greenhouse gas emissions in agriculture without compromising food security? *Environ. Res. Lett.* **12,** 105004 (2017).
31. Hejazi, M. I. *et al.* 21st century United States emissions mitigation could increase water stress more than the climate change it is mitigating. *Proc. Natl. Acad. Sci.* **112,** 10635–10640 (2015).
32. Wang, K., Yan, M., Wang, Y. & Chang, C.-P. The impact of environmental policy stringency on air quality. *Atmos. Environ.* **231,** 117522 (2020).
33. Weitzman, M. L. Can Negotiating a Uniform Carbon Price Help to Internalize the Global Warming Externality? *J. Assoc. Environ. Resour. Econ.* **1,** 29–49 (2014).
34. Cullenward, D. & Victor, D. G. *Making Climate Policy Work*. (John Wiley & Sons, 2020).
35. Green, J. F. Does carbon pricing reduce emissions? A review of ex-post analyses. *Environ. Res. Lett.* **16,** 043004 (2021).
36. Lee, D.-Y., Elgowainy, A., Kotz, A., Vijayagopal, R. & Marcinkoski, J. Life-cycle implications of hydrogen fuel cell electric vehicle technology for medium- and heavy-duty trucks. *J. Power Sources* **393,** 217–229 (2018).
37. Harper, A. B. *et al.* Land-use emissions play a critical role in land-based mitigation for Paris climate targets. *Nat. Commun.* **9,** 2938 (2018).

38. Sanchez, D. L., Johnson, N., McCoy, S. T., Turner, P. A. & Mach, K. J. Near-term deployment of carbon capture and sequestration from biorefineries in the United States. *Proc. Natl. Acad. Sci.* **115**, 4875–4880 (2018).
39. Kang, Y. *et al.* Bioenergy in China: Evaluation of domestic biomass resources and the associated greenhouse gas mitigation potentials. *Renew. Sustain. Energy Rev.* **127**, 109842 (2020).
40. Vohra, K. *et al.* Global mortality from outdoor fine particle pollution generated by fossil fuel combustion: Results from GEOS-Chem. *Environ. Res.* **195**, 110754 (2021).
41. Liu, S. *et al.* Spatial-temporal variation characteristics of air pollution in Henan of China: Localized emission inventory, WRF/Chem simulations and potential source contribution analysis. *Sci. Total Environ.* **624**, 396–406 (2018).
42. Lamontagne, J. R. *et al.* Large Ensemble Analytic Framework for Consequence-Driven Discovery of Climate Change Scenarios. *Earths Future* **6**, 488–504 (2018).
43. Calvin, K. *et al.* The SSP4: A world of deepening inequality. *Glob. Environ. Change* **42**, 284–296 (2017).
44. Hartin, C. A., Patel, P., Schwarber, A., Link, R. P. & Bond-Lamberty, B. P. A simple object-oriented and open-source model for scientific and policy analyses of the global climate system – Hector v1.0. *Geosci. Model Dev.* **8**, 939–955 (2015).
45. Environmental Sciences Division, O. R. N. L. Global, Regional, and National Fossil-Fuel CO2 Emissions. (2010) doi:10.3334/CDIAC/00001_V2010.
46. Kyle, G. P. *et al. GCAM 3.0 Agriculture and Land Use: Data Sources and Methods*. https://www.osti.gov/biblio/1036082 (2011) doi:10.2172/1036082.
47. Ou, Y. *et al.* Deep mitigation of CO2 and non-CO2 greenhouse gases toward 1.5 °C and 2 °C futures. *Nat. Commun.* **12**, 6245 (2021).
48. Rao, S. *et al.* Future air pollution in the Shared Socio-economic Pathways. *Glob. Environ. Change* **42**, 346–358 (2017).
49. Crippa, M. *et al.* Gridded emissions of air pollutants for the period 1970–2012 within EDGAR v4.3.2. *Earth Syst. Sci. Data* **10**, 1987–2013 (2018).

50. Krol, M. *et al.* The two-way nested global chemistry-transport zoom model TM5: algorithm and applications. *Atmospheric Chem. Phys.* **5,** 417–432 (2005).